8: UV (MeOH) λ_{max} 370, 254, 211, 208 nm; IR (KBr) 3029, 2980, 1658, 1454, 1377, 1264, 1032, 758, 702 cm^{-1}; ^1H NMR ($CDCl_3$) δ 7.32-7.17 (3H, Ph), 7.08 (d, 2H (ortho), Ph, *J*=8.0 Hz), 3.59 (dd, 1H (β) of CH, *J*=12.0 Hz, *J*=8.0 Hz), 2.58 (dd, 1H (α) of CH_2, *J*=12.0 Hz, *J*=8.0 Hz), 2.45 (dd, 1H (β) of CH_2, *J*=12.0 Hz, *J*=12.0 Hz), 2.10 (s, CH_3), 2.09 (s, CH_3), 1.23 (s, CH_3), 0.97 (s, CH_3); ^{13}C NMR ($CDCl_3$) δ 203.8, 200.1, 145.6, 145.5, 137.9, 128.2, 127.5, 126.7, 53.86, 48.42, 45.58, 33.43, 20.44, 13.52, 13.45, 13.44; Mass (EI) m/e 268 (M), 104 (100%).

9: UV (MeOH) λ_{max} 370, 254, 211, 208 nm; IR (KBr) 3029, 2980, 1658, 1454, 1377, 1264, 1032, 758,702 cm^{-1}; ^1H NMR ($CDCl_3$) δ 7.32-7.17 (3H, Ph), 6.99 (d, 2H (ortho), Ph, *J*=8.0 Hz), 3.63 (dd, 1H (α) of CH, *J*=12.0 Hz, *J*=8.0 Hz), 2.81 (dd, 1H (α) of CH_2, *J*=12.0 Hz, *J*=12.0 Hz), 2.26 (dd, 1H (β) of CH_2, *J*=12.0 Hz, *J*=8.0 Hz), 1.99 (s, CH_3), 1.69 (s, CH_3), 1.48 (s, CH_3), 1.46 (s, CH_3); ^{13}C NMR ($CDCl_3$)δ 201.3, 198.9, 145.8, 145.7, 144.9, 138.5, 128.1, 127.6, 126.9, 56.27, 47.98, 46.87, 34.80, 20.82, 18.00, 13.66, 12.95; Mass (EI) m/e 268 (M), 104 (100%).

11: UV (MeOH) λ_{max} 320, 308, 249, 211, 208 nm; IR (KBr) 3029, 2987, 1679, 1447, 1377, 1222, 1086, 758, 702 cm^{-1}; ^1H NMR ($CDCl_3$)δ 7.32-7.21 (2×3H, Ph), 6.96 (d, 2×2H (ortho), Ph, *J*=8.0 Hz), 3.73 (dd, 2×1H (β) of CH, *J*=12.0 Hz, *J*=8.0 Hz), 2.71 (dd, 2×1H (α) of CH_2, *J*=12.0 Hz, *J*= 8.0 Hz), 2.49 (dd, 2×1H (β) of CH_2, *J*=12.0 Hz, *J*=12.0 Hz), 1.50 (s, 2×CH_3), 1.06 (s, 2×CH_3); ^{13}C NMR ($CDCl_3$)δ 215.2, 137.4, 128.3, 127.1, 126.9, 56.78, 51.79, 43.47, 37.16, 22.63, 12.74; Mass (EI) m/e 372 (M), 268, 104 (100%).

12: UV (MeOH) λ_{max} 370, 241, 218, 211, 204 nm; IR (KBr), 3029, 2973, 1686, 1658, 1454, 1377, 1025, 899 cm^{-1}; ^1H NMR ($CDCl_3$) δ 7.43-7.06 (10H, Ph), 3.55 (1H of CH), 2.89 (1H of CH_2), 2.81 (1H of CH_2), 2.60 (1H of CH), 2.48 (1H of CH_2), 2.32 (1H of CH_2), 0.96 (s, CH_3), 0.74 (s, CH_3), 0.68 (s, CH_3), 0.64 (s, CH_3); ^{13}C NMR ($CDCl_3$) δ 213.2, 212. 7, 139.1, 137.7, 128.5-126.6 (Ph, overlapped), 54.64, 49.26, 48.49, 42.69, 37.44, 33.42, 22.40, 19.97, 19.96, 15.10; Mass (EI) m/e 372 (M), 268, 104 (100%).

13: ^1H NMR ($CDCl_3$) δ 7.34-6.93 (10H, Ph), 3.65 (1H of CH), 3.52 (1H of CH), 2.96 (1H of CH_2), 2.65 (1H of CH_2), 2.37 (1H of CH_2), 2.27 (1H of CH_2), 1.69 (s, CH_3), 1.62 (s, CH_3), 1.35 (s, CH_3), 0.71(s, CH_3); ^{13}C NMR ($CDCl_3$) δ 211.2, 208.3, 146.6, 146.5, 138.6, 138.4, 146.6-126.8 (Ph, overlapped), 61.22, 49.81 (CH), 49.49, 42.90 (CH), 35.54, 34.31, 23.48 (CH_3), 22.11 (CH_3), 19.13 (CH_3), 12.81 (CH_3); Mass (EI) m/e 372 (M), 268, 104 (100%).

14: UV (MeOH) λ_{max} 370, 357, 346, 245, 218, 212, 206 nm; IR (KBr) 3026, 2923, 1721, 1687, 1452, 1370, 908, 757, 700 cm^{-1}; ^1H NMR ($CDCl_3$) δ 7.07, 6.52, 2.20, 2.05, 1.83, 1.42 [polymer chain], and 2.33 (q, 1H), 1.42 (s, 2×CH_3), 1.26 (d, CH_3), 1.11 (s, CH_3) [duroquinone].

Acknowledgment. We appreciate the financial support of this work by the Organic Chemistry Research Center (OCRC) sponsored by the Korea Science and Engineering Foundation (KOSEF). This work was also supported (in part) by the Basic Science Research Institute Program, Ministry of Education, Project No. BSRI-97-3431.

References

1. Laird, T. In *Comprehensive Organic Chemistry*, Stoddart, J. F., Ed.; Pergamon Press: 1979; Vol. 1, pp 1213.
2. Maruyama, K.; Osuka, A. In *The Chemistry of the Quinonoid Compounds*, Part 1; Patai, S.; Rappoport, Z., Ed.; John Wiley & Sons: New York, 1988; Chapter 13, pp 759.
3. Bryce-Smith, D.; Fray, G. I.; Gilbert, A. *Tetrahedron Lett.* **1964**, *31*, 2137.
4. Kohn, H.; Li, V. S-; Schiltz, P.; Tang, M. S. *J. Am. Chem. Soc.* **1992**, *114*, 9218.
5. Kim, S. S.; Kim, A. R.; O, K. J.; Yoo, D. J.; Shim, S. C. *Chemistry Lett.* **1995**, 787.
6. In our previous results, **4** and **5** was prepared from the photoaddition reaction of **1** and diphenylacetylene. For spectral data of **4** and **5**, see Kim, S. S.; Kim, A. R.; Yoo, D. J.; Shim, S. C. *Bull. Korean Chem. Soc.* **1995**, *16*, 797.
7. Two other stereoisomers were also found, and similar patterns of UV, IR, ^1H NMR, ^{13}C NMR spectra were observed. Mass (EI) spectra were also obtained to confirm the molecular weight (m/e 372).

Effect of Au and WO_3 on the Surface Structure and Photocatalytic Activity of TiO_2

Wan In Lee*, Guang Jin Choi†, and Young Rag Do‡

**Department of Chemistry and Center for Molecular Dynamics, Inha University, Inchon 402-751, Korea*
†Division of Chemical Engineering, Korea Institute of Science and Technology, P.O. Box 131, Seoul 130-650, Korea
‡Samsung Display Devices Co., Suwon, Kyungki 445-970, Korea
Received March 11, 1997

Heterogeneous photocatalysis with titanium oxide (TiO_2) is a promising method for the decomposition of organic pollutants dissolved in water.[1-3] Previously, we have demonstrated that photocatalytic activity of TiO_2 can be greatly im-

proved by loading of some metals or metal oxides on its surface.[4-8] It has been found that a few metals such as Au, Ag or Pd can improve photocatalytic activity of TiO_2. Moreover, WO_3 or MoO_3 can increase photocatalytic activity of TiO_2 with even higher rate.

In this work, two surface-modified TiO_2 samples, that is, Au/TiO_2 and WO_3/TiO_2, were prepared and their kinetic parameters were determined with the Langmuir-Hinshelwood treatment. The difference of photocatalytic activity between Au/TiO_2 and WO_3/TiO_2 samples was discussed.

Experimental

A commercial form of TiO_2 (Degussa P25; surface area of 50 m^2/g) was chosen as a standard. Au/TiO_2 was prepared by the photodecomposition of $AuCl_3$ onto TiO_2. Preparation method is shown elsewhere.[9] WO_3/TiO_2 samples were prepared by the incipient wetness method. TiO_2 (Degussa, P25) was dispersed in H_2WO_4 (Allied Chemical & Dye Corporation) aqueous solution and dried in a water bath. Then, it was heat-treated at a rate of 100 °C/h up to 480 °C and held for 1 hour in a flowing oxygen.

1,4-dichlorobenzene (DCB) was utilized as a model compound for the evaluation of photocatalytic activity of prepared three TiO_2 samples. 15 mL of 0.0015 wt% ultrasonically dispersed photocatalyst sample was transferred to a Pyrex reactor and the stoichiometric amount of DCB aqueous solution was added. By adding water, total volume of the solution was adjusted to 30 mL and concentration of DCB to 10~100 PPM. Samples were then irradiated with a 150 watt xenon lamp. After the irradiation of every 2.5 min, the concentration of remnant DCB in the solution was measured with a Perkin-Elmer 552A UV-visible spectrophotometer.

The surface acidity was evaluated by titrating 0.5 g of WO_3/TiO_2 powders suspended in benzene with 0.1 N n-butylamine benzene solution, using methyl red as indicator.[10]

Results and Discussion

The decomposition reaction of DCB with each TiO_2 sample approximated to first-order kinetics. Hence, the photocatalytic activity was defined and compared in terms of overall degradation rate constant. It was found that for Au/TiO_2 the optimum concentration of Au providing the maximized photocatalytic efficiency was 0.5 mole percent relative to TiO_2 and that of WO_3 was 3.0 mole percent for WO_3/TiO_2. At this optimized loading concentration, the photocatalytic activities of Au/TiO_2 and WO_3/TiO_2 samples are 2.0 times and 2.5 times respectively compared to that of pure TiO_2, as given in Table 1. The decomposition of 1,4-dichlorobenzene as a function of irradiation time with each TiO_2 sample is described in Figure 1.

Table 1. Photocatalytic activities and kinetic parameters of several

Sample	Photocatalytic activity (Overall degradation rate constant, min^{-1})	k ($\mu M\ min^{-1}$)	K (μM)
Pure TiO_2	0.012	3.3	0.026
1.5 mole % Au/TiO_2	0.024	9.5	0.010
3.0 mole % WO_3/TiO_2	0.030	7.3	0.024

During the photocatalytic process, the absorption of a photon by TiO_2 leads to the promotion of an electron from the valence band to the conduction band and thus produces an electron-hole pair. The electron in the conduction band is removed by reacting with oxygen dissolved in water, and the hole in the valence band can react with OH^- or H_2O species, which are adsorbed on the surface of TiO_2, to give the hydroxyl radical.[11] It has been proposed that the produced hydroxyl radical initiates various oxidation reactions. The electron-hole recombination process is in direct competition with space charge separation of electron and hole. The photocatalytic activity of TiO_2 will be enhanced by retarding the electron-hole recombination and a principal method of slowing electron-hole recombination is thought to be through the loading of conductive material onto the TiO_2 surface. Accordingly, dispersed metal, such as Au, on TiO_2 surface can expedite the transport of photoexcited electrons to outer system. The same argument can also be applied to WO_3/TiO_2 samples. Tennokone *et al.* reported that the W (VI) in WO_3 can be easily reduced to W (V).[12] Hence, it is deduced that in the presence of WO_3 the electrons in the conduction band of TiO_2 are accepted by WO_3, resulting in the formation of W (V). These electrons in tungsten oxide will then be transferred to outer oxygen adsorbed on the surface of TiO_2, and the reduced form of tungsten oxide will return back to original WO_3.

From a electron-transfer efficiency point of view, Au will be much more efficient than WO_3. However, as shown in Figure 1, WO_3/TiO_2 exhibits higher photocatalytic activity than Au/TiO_2 toward the oxidation of 1,4-dichlorobenzene. It is indicated that the electron transfer rate is not unique factor in determining the photocatalytic activity. Possibly, microstructure of TiO_2 surface might be an another crucial factor.[13]

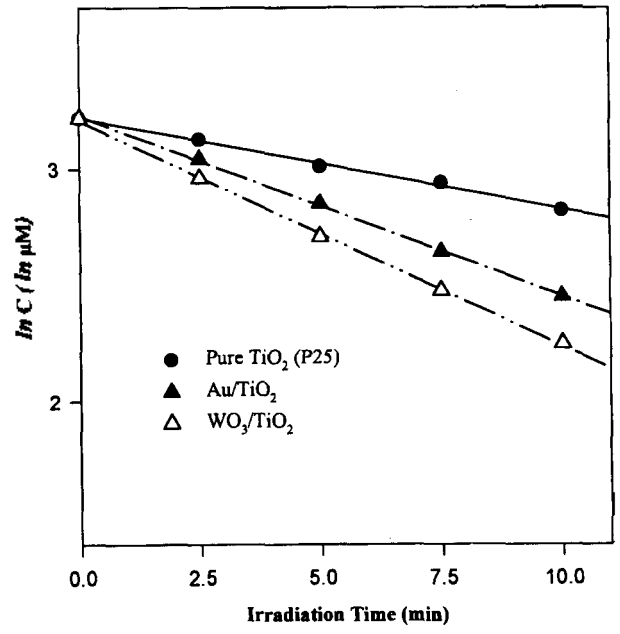

Figure 1. Decomposition of DCB vs. irradiation time with several suspended TiO_2 samples (Initial DCB concentration : 25 μM).

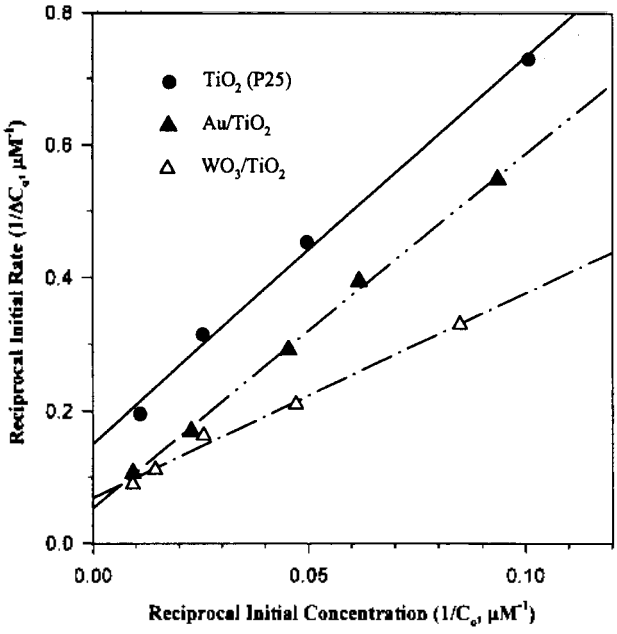

Figure 2. Concentration dependence of initial reaction rate (Initial DCB concentration : 10-100 μM).

Langmuir-Hinshelwood kinetic treatment was introduced to analyze the kinetic parameters for the three TiO_2 samples. From the traditional derivation of Langmuir-Hinshelwood kinetic, **K** represents the equilibrium adsorption constant, while ***k*** reflects the reaction rate constant, that is, a measure of intrinsic reactivity at the surface of catalyst. The rate of reaction (r) can be expressed by

$$r = kKC/(1 + KC)$$

At an initial concentration (C_o), above equation can be modified to

$$1/r_o = 1/k + 1/(kKC_o)$$

Initial reaction rate (r_o) can be measured simply by

$$r_o = (C_o - C)/\Delta t$$

, where **C** is the concentration of reactant after a given time interval (Δt).

In this experiment, Δt was chosen to 2 min and the initial concentration of DCB (C_o) was varied from 10 to 100 PPM. By plotting $1/C_o$ vs. $1/r_o$ as shown in Figure 2, the reaction rate constants (***k***) and equilibrium binding constants (**K**) of three TiO_2 samples were determined (Table 1). Compared to standard TiO_2, Au/TiO_2 demonstrates about three times higher reaction rate constant, while the equilibrium binding constant is less than a half. It is considered that the high reaction rate constant of Au/TiO_2 sample originates from the efficient electron transfer via Au on the surface of TiO_2. On the contrary, Au clusters on TiO_2 surface may make a detrimental effect to the photocatalytic reaction, since the active sites on TiO_2 surface might be screened by the loaded Au clusters. This explains why Au-loaded TiO_2 sample beholds relatively small equilibrium binding constant. WO_3/TiO_2 sample also shows highly increased reaction rate constant, but it is comparatively lower than that of the Au-loaded TiO_2 sample, as expected. However, the equilibrium

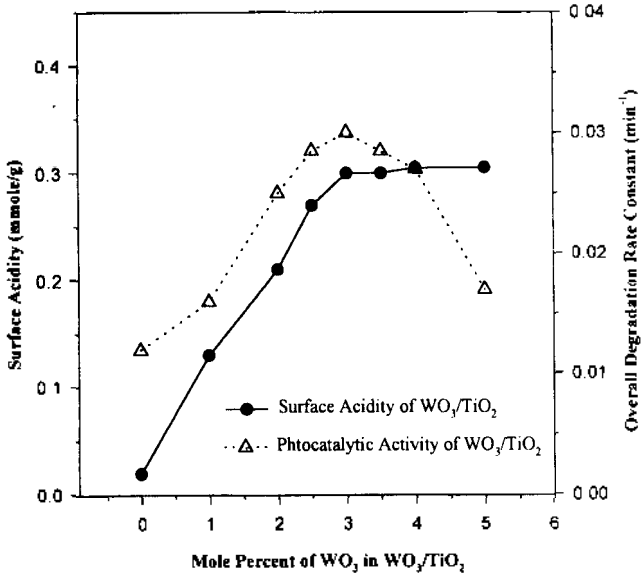

Figure 3. Surface acidity and photocatalytic activity of WO_3/TiO_2 with the loaded WO_3 concentration.

binding constant of WO_3/TiO_2 samples is virtually the same as that of pure TiO_2, quite differently from Au/TiO_2 sample. This implies that active sites of TiO_2 are not influenced at all by the loading of WO_3.

In order to investigate the surface state of WO_3/TiO_2, surface acidity was measured as a function of loaded WO_3 concentration. Since WO_3 retains much higher surface acidity value than TiO_2, surface acidity of WO_3/TiO_2 will be increased by increasing the WO_3 concentration, until all of TiO_2 surface is covered with WO_3. As shown in Figure 3, surface acidity was increased steadily but it reached a plateau level from approximately 3 mole percent of WO_3 in WO_3/TiO_2. This indicates that at least 3 mole percent of WO_3 is needed to cover the TiO_2 surface completely. It has been reported that 3.4 mole percent of WO_3 is necessary to cover the surface of Degussa P25 (50 m^2/g) by monolayer thickness.[14] Therefore, it is derived that in the prepared WO_3/TiO_2 sample, WO_3 covers the surface of TiO_2 with monolayer thickness and the photocatalytic activity is maximized at this coverage. Monolayer coverage of WO_3 will not change the surface structure of TiO_2 and this explains why the equilibrium binding constant is the same as that of pure TiO_2 and why WO_3/TiO_2 is more efficient than Au/TiO_2 in the photocatalytic decomposition of DCB.

Acknowledgment. This research was supported by Inha University.

References

1. Hoffmann, M. R.; Martin, S. T.; Choi, W.; Bahnemann, D. W. *Chem. Rev.* **1995**, *95*, 69.
2. Turchi, C. S.; Ollis, D. F. *J. Catal.* **1990**, *122*, 178.
3. Serpone, N. *Sol. Energy Mater. Sol. Cells* **1995**, *38*, 369.
4. Gao, Y-M.; Lee, W.; Trehan, R.; Kershaw, R.; Dwight, K.; Wold, A. *Mater. Res. Bull.* **1991**, *26*, 1247.
5. Lee, W.; Shen, H-S.; Dwight, K; Wold, A. J. *Solid State Chem.* **1993**, *106*, 288.
6. Wang, C-M.; Heller, A.; Gerischer, H. *J. Amer. Chem.*

Soc. **1992**, *114*, 5230.
7. Lee, W.; Do, Y. R.; Dwight, K.; Wold, A. *Mater. Res. Bull.* **1993**, *28*, 1127.
8. Do, Y. R.; Lee, W.; K. Dwight; Wold, A. *J. Solid State Chem.* **1994**, *108*, 198.
9. Albert, M.; Gao, Y-M.; Toft, D.; Dwight, K.; Wold, A. Mater. *Res. Bull.*, **1992**, *27*, 961.
10. Tanbe, K.; Ishiya, C.; Matsuzaki, I.; Ichikawa, I.; Hattori, H. *Bull. Chem. Soc. Japan*, **1972**, *45*, 47.
11. Gerischer, H.; Heller, A. *J. Phys. Chem.* **1991**, *95*, 5261.
12. Tennakone, K.; Heperuma, O. A.; Bandara, J. M. S.; Kiridena, W. C. B. *Semicond. Sci. Technol.* **1992**, *7*, 423.
13. Bickley, R. I.; Gonzalez-Carreno, T.; Lees, J. S.; Palmisano, L.; Tilley, R. J. D. *J. Solid State Chem.* **1991**, *92*, 178.
14. Hilbrig, F.; Gel, H. E.; Kninger, H.; Schmelz H.; Lengeler, B. *J. Phys. Chem.* **1991**, *95*, 6973.

Synthesis and Crystal Structure of Bis[(η^5-Cp)tris-(dimethylphosphito-P)cobalt-O,O',O'']acetylacetonato]Yttrium(III)

Kyung-Chae Kim, Yu-Chul Park, and Jong Hwa Jeong*

Department of Chemistry, Kyungpook National University, Taegu 702-701, Korea
Received March 15, 1997

Homoleptic β-diketonato complexes of yttrium have been extensively studied, which are useful precursors for Y123 superconducting material due to high vapor pressure.[1] However, heteroleptic yttrium complexes of β-diketonatonate are rare.[2] In our laboratory, yttrium complex containing O-donor tripodal ligands (L=CpCo[P(O)(OMe)$_2$]$_3$), L_2YCl, has been used to prepare an acetato complex of YL_2, in which the acetate ligand has been bound to yttrium ion in an isobidentate type to form four-membered ring.[3] This result implies the ligand L is bulk enough to prevent formation of polynuclear yttrium complex. Therefore, this fact has prompted us to investigate the chemical bonding behavior of acetylacetonato (acac) ligand toward YL_2 moiety since the ligand is more crowded than acetate and able to form six-membered ring. Here we wish to report the synthesis and X-ray structure of an acetylacetonato complex of YL_2.

Experimental

Solvents were purified by standard methods and were freshly dried and distilled prior to use. Potassium acetylacetonate hemihydrate was purchased from Aldrich Co. and dried using P_2O_5. NaL was prepared by the literature method.[4] All manipulations were performed under an argon atmosphere using a double manifold vacuum system and Schlenk techniques at room temperature.

^{1}H and ^{13}C NMR spectra were obtained in $CDCl_3$ and referenced to the deuterated solvent (δ 7.14 ppm for ^{1}H, 77.0 ppm for ^{13}C) on a Bruker AM-300 spectrometer. FT-IR spectrum was obtained on a Bomen Michelson 100 spectrometer as KBr pellet. Chemical analyses were carried out by the Chemical Analysis Laboratory at Korea Basic Science Institute.

Preparation of L_2 (acac) Y. 20 mL of dry THF was introduced to a mixture of 0.49 g (1.0 mmol) of NaL and 0.10 g (0.5 mmol) of YCl_3. The mixture was stirred at room temperature for 24 h resulting yellow solution and precipitate. The solution was transferred to 0.07 g (0.5 mmol) of potassium acetylacetonate in 20 mL of THF. The resulting suspension was stirred at room temperature for 2 days and then the precipitate was filtered off. The filtrate was evaporated *in vacuo* to afford yellow solid. Recrystallization of the crude product from THF solution gives yellow crystals in 75% yield (0.4 g).

Analysis : Calcd. (%) C; 30.68, H; 5.46 Found (%) C; 30.52, H; 5.37.

^{1}H NMR ($CDCl_3$) : δ 5.30 (s, -COCH=C-, 1H) δ 4.99 (s, $2C_5H_5$, 10H), δ 3.74 (m, $12H_3C$-O-P, 36H), δ 1.90 (s, H_3CCO-, 6H)

^{13}C NMR ($CDCl_3$) : δ 186.2 (s, C=O), δ98.4 (s, CH=), δ 88.8 (s, C_5H_5), δ 51.3 (m, H_3COP), δ 27.3 (s, H_3C-)

IR (cm^{-1}) : 2943 (m), 2837 (w), 1620 (m), 1513 (m), 1462 (w), 1263 (m), 1016 (vs)

X-ray crystallographic analysis. An X-ray quality single crystal, 0.30×0.30×0.50 mm, was mounted in a thin-walled glass capillary on an Enraf-Nonius CAD-4 diffractometer with Mo-Kα radiation (λ=0.71073 Å). Unit cell parameters were determined by least-squares analysis of 25 reflections (10°<θ<13°). Intensity data were collected with θ range of 3.29-30.40° in ω/2θ scan mode. Three standard reflections (h k l = 5 −7 3; 5 7 6; −3 −2 8) were monitored every 1 hr during data collection, which was showing not significant variation. The data were corrected for Lorentz-polarization effects and decay. Empirical absorption corrections with Ψ scans were applied to the data. The structure was solved by using Patterson method and refined by full-matrix least-squares techniques on F^2 using SHELXS-86[5] and SHELXL-93.[6] All non-hydrogen atoms were refined by using anisotropic thermal factors, and all hydrogen atoms were positioned geometrically using riding model with 1.2 times isotropic thermal factors of the attached non-hydrogen atoms. The final cycle of the refinement con-